*AppliedChem*

MDPI

*Article*

# On Over-Parameterisation and Parameter Estimation of Enzyme Kinetics

**Thomas Waluga * and Paras Nagshi**

Institute of Process Systems Engineering, Hamburg University of Technology, 21073 Hamburg, Germany
* Correspondence: thomas.waluga@tuhh.de

**Abstract**

The estimation of kinetic parameters based on experiments is an important element in understanding the reaction mechanisms of enzymes and their intrinsic properties. However, increasing model complexity by introducing multiple parameters can lead to overparameterisation, resulting in poor parameter identifiability and potentially causing the model to describe noise rather than underlying biochemical mechanisms. In this study, we use the total quasi-steady-state assumption to clarify whether the parameters of multi-parameter models can be correctly identified even with a high number of parameters. Therefore, a basic model was used, and the number of parameters was increased successively. A Bayesian optimisation approach was applied, which predicted the next experiments with the highest information density in order to reduce the experimental effort required for the experiments. The results show, on the one hand, that the parameters of multi-parameter models can indeed be correctly identified. On the other hand, it also shows that under certain conditions, incorrect values were estimated, even though the consideration of confidence intervals suggested correct identification.

**Keywords:** biocatalysis; progress curve analysis; parameter estimation

## 1. Introduction

Biotechnology is a key enabling element in the transition of the chemical industry toward sustainable processes. Accordingly, the share of biotechnological products in the chemical industry has steadily increased over the past few decades [1,2]. The advantages of biotechnological processes are evident: their high selectivity generally results in lower waste generation, particularly for complex molecules; the use of water as a solvent supports sustainability; and optimal operating conditions are typically achieved under mild conditions, leading to reduced energy demand [3]. Despite these advantages, biotechnological processes must also remain economically competitive with conventional routes. In this context, process intensification provides an opportunity to increase the efficiency of biotechnological processes and to enhance their economic attractiveness [3]. In particular, computer-aided methods offer substantial potential [4], with process modelling being especially important [5], as it enables the systematic development and optimisation of processes [6].

The core of any model is the mathematical description of the individual unit operations. In biocatalysis, this applies in particular to enzyme kinetics. A correct description of enzyme kinetics enables the identification of optimal process conditions [7]. In addition, such a description provides insight into the reaction mechanism, which is essential for both the course of the reaction and its mechanistic interpretation [8].



Academic Editor: Philippe Michaud

Received: 28 January 2026
Revised: 23 February 2026
Accepted: 7 April 2026
Published: 9 April 2026

The most fundamental enzymatic rate expression is the Michaelis–Menten equation, as given in Equation (1):

$$-\frac{d[A]}{dt} = \frac{[E]_{tot} k_{cat} [A]}{K_M + [A]} \quad (1)$$

where [A] represents the concentration of the substrate, $[E]_{tot}$ represents the amount of enzyme, $k_{cat}$ represents the catalytic constant, and $K_M$ denotes the Michaelis constant, representing the affinity of the substrate. This equation represents the differential form of an enzyme-kinetic model. A widely used method to obtain data for parameter estimation according to Equation (1) is initial rate experiments [9]. These experiments are simple and robust. However, they rely on simplifying assumptions, and their interpretability must therefore be treated with caution. These limitations include [10–12]: the assumption of negligible substrate depletion and product formation during the measurement; the neglect of reverse reaction contributions; sensitivity to pipetting/mixing dead time and the choice of the fitting window, which can introduce systematic errors; and the fact that initial rates often provide limited information content, making parameter estimation less identifiable and more susceptible to correlated parameters, especially when more complex mechanisms are considered.

As an alternative approach, progress curve analysis can be performed [13–16]. This more closely reflects the actual reaction conditions. However, they come with different challenges, primarily of a mathematical nature. In particular, parameter estimates obtained from progress curves can depend on the numerical method used to integrate the differential model equations [13]. Moreover, the results can be strongly influenced by the initial parameter values supplied to initialise the iterative optimisation algorithm [13,17,18].

Equally important as the experimental approach used to determine kinetic parameters is an understanding of the reaction mechanism [8]. The classical Michaelis–Menten equation (Equation (1)) assumes an irreversible uni–uni mechanism. Most real reaction mechanisms, however, are substantially more complex. Many reactions require two or more substrates, inhibition by substrates or products may occur, and equilibria can limit conversion in closed systems, independent of whether the reaction is studied in the forward or reverse direction [8]. This increases the number of parameters and may therefore appear to make identification of the correct parameter set more challenging. In practice, however, the naïve application of complex models often seems to "work" surprisingly well. This is because additional parameters increase model flexibility, allowing the model to adapt more easily to experimental data [19]. If the quality of a parameter estimate is assessed using simple goodness-of-fit criteria such as the coefficient of determination ($R^2$), seemingly suitable parameters can be obtained easily, yet they may be determined with insufficient precision or even with good precision but not reflecting the intrinsic characteristic of the enzyme. To complement this metric, the normalised root mean square error (nRMSE) was calculated, providing a more sensitive measure of deviations between simulated and reference data.

The literature contains several examples of enzyme-kinetic models that employ a comparatively large number of parameters to describe enzyme kinetics. The majority of these models concern lipase-catalysed esterification or transesterification reactions, typically described by ordered bi–bi or ping–pong-type mechanisms including multiple inhibition terms. García et al. [20] propose, by their account, a generally applicable mechanism for an esterification reaction catalysed by an immobilised lipase, comprising a total of 13 parameters. Their study investigated the esterification of long-chain fatty alcohols and acids. Overall, García et al. consider, for their reference systems, both forward and reverse reactions, as well as uncompetitive inhibition by all components and competitive inhibition by the alcohol, the acid, and the ester. The proposed rate equation implies an ordered mechanism in which the acid preferentially binds to the enzyme as the first

substrate. In another example, Yadav and Devi [21] propose an 11-parameter reaction mechanism for the transesterification of ethyl butyrate and tetrahydrofurfuryl alcohol catalysed by a lipase, in which five inhibition terms are considered in addition to forward and reverse reactions. Other examples from the literature for lipase-catalysed esterification employ, for instance, models with six [22] or five [23,24] parameters. However, also critical studies do exist: van Hecke et al. [25] propose a substantially simpler second-order model for the lipase reaction, as the confidence intervals calculated from their measurements indicate non-identifiability of classical Michaelis–Menten parameters and thus suggest over-parameterisation. A similar approach to model simplification is also recommended by Heeres et al. [26], likewise on the basis of non-identifiability. This situation is referred to as over-parameterisation or sloppiness, i.e., a kinetic model contains more (or overly flexible) parameters that cannot be uniquely determined from the available measurement data. As a result, excellent fits may be achieved, while the parameter values are neither unique nor mechanistically representative of the intrinsic characteristics of the enzymes [19].

It was already recognised in earlier studies [27] that, in progress curve analysis using the simple Michaelis–Menten kinetics as an example, the standard quasi-steady-state assumption (sQSSA) allows the ratios of $k_{cat}$ and $K_M$ to be estimated reliably, whereas the exact parameter values are difficult to determine and, in many cases, cannot be identified uniquely without substantial experimental and computational effort. It is therefore entirely appropriate to determine the quotients directly [28]. In this context, it has been shown that adopting the total quasi-steady-state approach (tQSSA) can be used successfully to enhance the parameter identifiability and to enable unique parameter estimation. The tQSSA extends the classical sQSSA framework by formulating the dynamics in terms of total variables [29], most notably the total substrate ($[A]_{tot} = [A] + [EA]$) (free substrate A plus enzyme–substrate complex EA), rather than relying on the free substrate concentration alone [30]. In the sQSSA, the central assumption is that the enzyme–substrate complex rapidly relaxes to a quasi-steady state, i.e., ($d[EA]/dt \approx 0$). This approximation is typically accurate when the total enzyme concentration is small compared with the relevant substrate scale, commonly expressed as $[E]_{tot} << [A]_0 + K_M$. The sQSSA approach does not require substrate depletion to be negligible, although in practice, sQSSA is often combined with initial-rate measurements where substrate and product changes are small. In contrast, the tQSSA assumes $[A]_{tot}$ as the primary variable and thereby accounts explicitly for enzyme sequestration, which becomes relevant when the enzyme is not negligible relative to the substrate. Consequently, tQSSA can remain accurate in regimes where $[E]_{tot}$ is comparable to $[A]_0$ [31], in which case the sQSSA may lose accuracy. From a data-analysis perspective, using tQSSA-based formulations can lead to numerically better-conditioned model equations for progress-curve fitting and may improve the practical identifiability of the kinetic parameters [30]. However, it does not create additional information; identifiability remains determined by the experimental design, the measurement noise, and the structural properties of the chosen model.

So far, it has been successfully demonstrated that the unique identification of $k_{cat}$ and $K_M$ according to Equation (1) by the application of the tQSSA approach is possible [27]. However, it is unknown if this identifiability is also possible for more complex reaction mechanisms. Within the present study, we will demonstrate the application of the tQSSA approach for complex reaction mechanisms and address the question of when over-parameterisation begins and which parameters can still be identified uniquely by the use of tQSSA. To this end, we consider the example of an irreversible two-substrate kinetics according to Equation (2) following a ping-pong mechanism, which is often used in the literature to describe, e.g., the reaction of a lipase [21–24].

$$-\frac{d[A]}{dt} = -\frac{d[B]}{dt} = \frac{[E]_{tot} k_{cat} [A][B]}{(K_{M,A}[B]) + (K_{M,B}[A]) + ([A][B])} \quad (2)$$

This comparatively simple kinetic model comprises three parameters that fully describe the system: $k_{cat}$, $K_{M,A}$, and $K_{M,B}$. The ping-pong mechanism involves two substrates (A, B) where the first substrate (A) binds to the enzyme, transfers a group to the enzyme (E), releases product, and leaves the enzyme modified (E*). Then the second substrate (B) binds to E*, accepts the group, releases the product, and regenerates the original enzyme (E). The rate expression can be extended in a modular manner to account for different reaction mechanisms. For example, if a mechanism is assumed where substrate A must bind to the enzyme first, competitive inhibition of B with respect to A can occur. This effect can be represented by the inhibition constant $K_{IC,B}$, which modifies the term ($K_{M,A}$ [B]) in the denominator by introducing the factor (1 + [B]/$K_{IC,B}$) [11,32]. Analogously, competitive inhibition can occur on the modified enzyme (E*) by the substrate (A), which is described by introducing the factor (1 + [A]/$K_{IC,A}$) to the term ($K_{M,B}$ [A]) [32]. If uncompetitive inhibition by A or B to the enzyme–substrate complex is assumed, it modifies the denominator term ([A][B]) by multiplication with (1 + [A]/$K_{IU,A}$) or (1 + [B]/$K_{IU,B}$), respectively [33]. If water acts as the second substrate, as in hydrolytic reactions, its concentration can be considered constant and effectively non-limiting. Under these conditions, the Ping-Pong Bi-Bi mechanism reduces to a pseudo-uni-bi reaction scheme, and the resulting kinetic parameters must be interpreted as apparent parameters that lump contributions from both half-reactions.

For the simple irreversible two-substrate kinetics according to Equation (2), these modular extensions yield 16 distinct model variants, while product inhibition and reversible reaction steps are not considered at this stage. Using this setting, the present study aims to demonstrate how many parameters can still be identified reliably and at which point over-parameterisation—or, more critically, mis-parameterisation—sets in. To this end, we employ in silico studies, as they allow the true kinetic parameters of an enzyme to be defined unambiguously.

## 2. Materials and Methods

Our study comprises two key steps. First, two in silico progress curves of the concentrations [A] and [B] are generated for different initial concentrations using pre-defined kinetic parameter values. In the subsequent step, the kinetic parameters are estimated by bounded nonlinear least-squares fitting (log-parameterisation), and two new initial concentrations are proposed to improve parameter identifiability by a Bayesian approach. Using these newly suggested initial concentrations, additional progress curves of [A] and [B] are generated, and the procedure is iterated accordingly. Each in silico progress curve consists of ten data points. Overall, up to ten iteration rounds are performed, resulting in a maximum of twenty experiments. Our methodology is illustrated by Scheme 1. All code is generated in Python 3.12.3 and is openly available in our repository (cf. data availability statement). The code generation itself was supported by the use of ChatGPT 5.2 Thinking.

The kinetic parameters considered in this study are defined according to Table 1. We acknowledge that these values do not necessarily correspond to a specific real-world system. However, when using in vitro experimental data, the true parameter values as well as the reaction mechanism are likewise unknown, such that the success of parameter estimation cannot be rigorously validated. The aim of this study is not to characterise enzyme kinetics, but to demonstrate to what extent it is possible to successfully identify (the true) intrinsic characteristics of an enzyme under the given conditions.

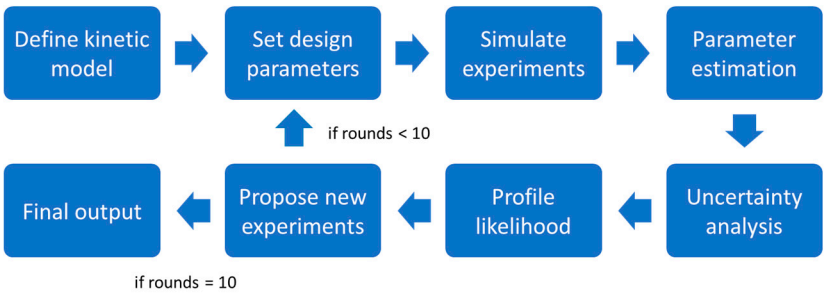


**Scheme 1.** Flow diagram of the iterative modelling and experimental design workflow applied in this study.

**Table 1.** Kinetic parameters used for this study.

| $k_{cat}$ | $K_{M,A}$ | $K_{M,B}$ | $K_{IC,A}$ | $K_{IC,B}$ | $K_{IU,A}$ | $K_{IU,B}$ |
|---|---|---|---|---|---|---|
| 5 $s^{-1}$ | 10 mM | 25 mM | 50 mM | 60 mM | 70 mM | 80 mM |

For the initial conditions, the concentrations $[A]_0$, $[B]_0$, and $[E]_{tot}$ can be specified. For all experimental series, these were chosen as listed in Table 2. The simulation of the progress curves according to Equation (2), as well as the modularly implemented inhibition expressions, was performed using a second-order Runge–Kutta method (explicit midpoint) with adaptive sub-stepping between measurement times. Simulated measurements were perturbed with normally distributed noise with σ = 1 mM, while negative concentrations were excluded by setting them to zero.

**Table 2.** Initial conditions for the initial experiments for all case studies.

| Experiment | $[E]_{tot}$ | $[A]_0$ | $[B]_0$ |
|---|---|---|---|
| 1 | 1 mM | 1 mM | 1 mM |
| 2 | 10 mM | 20 mM | 10 mM |

For a given set of experiments, each experiment i provides measured time points $t_{ij}$ and noisy observations ($A_{obs,ij}$ and $B_{obs,ij}$). For a candidate parameter vector θ, the model predicts $A_{pred,ij}(\theta)$ and $B_{pred,ij}(\theta)$ by simulating the progress curve. Accordingly, parameter estimation is performed by minimising the weighted residual sum of squares over all experiments and both observables, as given in Equation (3):

$$\min_{\theta} \sum_{i,j} \left( \frac{[A]_{pred,ij}(\theta) - [A]_{obs,ij}}{\sigma} \right)^2 + \sum_{i,j} \left( \frac{[B]_{pred,ij}(\theta) - [B]_{obs,ij}}{\sigma} \right)^2 \quad (3)$$

In the implementation, the residual vector is constructed by linking the [A] residuals and [B] residuals across all experiments. To enforce positivity and improve numerical robustness, the optimisation is carried out in log-parameter space with $x = \log(\theta)$ and $\theta = \exp(x)$ to avoid negative parameters. The objective is then minimised using *scipy.optimize.least_squares* with the trust-region reflective algorithm under explicit bounds in log-space. Tight termination tolerances are used with a maximum of 350 function evaluations. It is well known that the result of a parameter estimation depends on the initial parameters and the method used [13,17,18]. In our study, we assume that no prior knowledge of the true parameters is available. We therefore initiate the estimation with parameter values of 1 mM each, as this is often the default value used in commercial software.

After the initial experiments are specified as given by Table 2, each subsequent round proposes two new experimental conditions using a model-informed design criterion. First, admissible ranges for the decision variables $[A]_0$, $[B]_0$, and [E] are defined, and a finite candidate pool is generated within these bounds. For each candidate condition, the current model fit and its parameter uncertainty are used to predict how informative that experiment would be, following the decision-theoretic view of Bayesian experimental design [34]. Local sensitivities of the predicted measurements with respect to the parameters are approximated numerically to construct a Fisher information measure for each candidate [35]. This candidate information is then combined with the current uncertainty via a Laplace/Gaussian approximation around the fitted parameters to approximate how much the overall parameter uncertainty would shrink if the candidate experiment were performed, and candidates are ranked by a D-optimal objective by maximising the expected reduction in the uncertainty [35]. Finally, two experiments are selected, updating the expected precision after the experiments done before, so that the two new experiments add complementary information.

After convergence, an approximate covariance matrix in log-space is computed from the Jacobian J returned by *least_squares* via $\mathrm{Cov}(x) \approx (J^\top J)^\dagger$, using a pseudo-inverse. Standard errors (SE) are taken as the square roots of the diagonal entries. Two-sided 95% intervals are then computed as $\hat{x} \pm 1.96\,\mathrm{SE}$, clipped to a finite range for numerical stability, and exponentiated back to obtain confidence intervals on the original parameter scale. This approach is often used as it is computationally fast, but it relies on asymptotic normality and a well-approximated quadratic objective near the optimum. In strongly nonlinear models, with parameter bounds or strong parameter correlations, as is often reported for enzyme kinetics, it can underestimate or misrepresent uncertainty and tends to produce overly symmetric intervals as alternative likelihood profiles are calculated. Here, one parameter at a grid of values is fixed, and the remaining "nuisance" parameters are re-optimised, accepting values for which the likelihood deterioration $\Delta(-2\log L)$ remains below the cut-off $X^2_{1,0.95}$ (numerically about 3.84). The profile statistic is computed from the increase in the sum of squared errors relative to the MAP fit, according to Equation (4):

$$\phi(x) = \frac{\mathrm{SSE}(x) - \mathrm{SSE}(\hat{\theta})}{\sigma^2} \tag{4}$$

## 3. Results

For the selected model system, an irreversible two-substrate kinetics without any influence of products on the reaction, different reaction mechanisms can be postulated due to the possible occurrence of substrate-induced inhibition effects. The simplest mechanism is a reaction without inhibition, for which the model is defined by three parameters. The most complex case comprises four inhibition effects occurring simultaneously, resulting in a model with seven parameters. Although it is unlikely in practice that all four inhibition mechanisms are present at the same time, this scenario is sufficient for a systematic analysis. This is particularly justified given that the literature reports models with up to 13 parameters [20] when product effects and the reverse reaction are included.

According to the FAIR principle, all results can be reproduced by any person by running the Python files in our repository (cf. data availability statement). Since an evaluation is carried out after each round, any interested researcher can independently compile interim results. However, there is a marginal stochastic element, as noise is introduced in a random manner. In the code, the seed for the random noise is set so all "random" results are reproducible. Alternatively, the seed can be set to a random value itself, so slight differences may occur when re-running our code. In our repository, we provide all 16 candidates of the various combinations of substrate inhibitions that occur.

However, only nine candidates are presented in the case studies. Researchers are free to investigate candidates not covered here independently using our code. To facilitate a clearer understanding of the dynamic behaviour of the different case studies, representative time-course data from the 20th experiment of each case study scenario are provided in the Supplementary Materials. These curves illustrate the characteristic progression.

### *3.1. Case Study 1: No Inhibition, Described by Three Parameters*

The first case study under investigation is the simplest one. No inhibitions are assumed, and the model is defined by the three parameters, $k_{cat}$, $K_{M,A}$, and $K_{M,B}$. The reaction rate can be described by Equation (2). Table 3 reports the estimated parameters together with their confidence intervals as well as the value for the coefficient of determination ($R^2$).

**Table 3.** Parameters estimated in various rounds for a reaction without inhibition. Values in brackets represent the lower and upper limits of the 95% confidence interval.

| Round No. | $k_{cat}$ [$s^{-1}$] | $K_{M,A}$ [mM] | $K_{M,B}$ [mM] | $R^2$ [-] | nRMSE [-] |
|---|---|---|---|---|---|
| 1 | 1.35 [0.94, 1.92] | 2.17 [0.16, 29.36] | 0.001 [$1.93 \times 10^{-22}$, $5.18 \times 10^{21}$] | 0.98 | 0.1782 |
| 2 | 5.01 [4.99, 5.02] | 9.44 [8.49, 10.49] | 25.90 [24.76, 27.09] | 1.00 | 0.0058 |
| 10 | 5.00 [4.99, 5.01] | 9.95 [9.63, 10.28] | 25.07 [24.73, 25.41] | 1.00 | 0.0017 |

For the simplest 3-parameter model, the first round, which represents two experiments, yields parameter estimates that deviate strongly from the true values and exhibit very wide confidence intervals. Furthermore, the width of the confidence intervals, especially that for $K_{M,B}$, indicates a bad parameter estimation. In the second round, when two more experiments are performed, a clear transition occurs, with estimates close to the true values. The narrow confidence intervals indicate a good parameter estimation. From rounds 3 to 10, the estimates remain stable with parameters changing only marginally, and there is no additional gain. The $R^2$ values, which indicate the goodness-of-fit of the model to the experimental data, increased from 0.98 in round 1 to 1.00 from round 2 onward. In round 1, $R^2$ was already high, indicating a good fit (if un-reflected used), despite the parameter estimates deviating strongly from the true values. The nRMSE value decreases sharply between the first and second rounds and then continues to decrease in small steps with each subsequent round.

The profile likelihood plots shown in Figure 1 correspond to round 10 for all three parameters, $k_{cat}$, $K_{m,A}$ and $K_{m,B}$. The dotted line indicates the cut-off $X^2_{1,0.95}$ for the 95% confidence interval. Each profile exhibits a single, sharp minimum located close to the true parameter value with a steep rise on both sides of the minimum and extremely narrow confidence intervals below the threshold line. Profile likelihood plots from earlier rounds show behaviour that is consistent with the corresponding parameter estimates reported in Table 3.

### *3.2. Case Study 2: One Inhibition Described by Four Parameters*

This subchapter handles the common case of one inhibition by one of the two substrates. The inhibition can either be competitive to the enzyme E or modified enzyme E* or uncompetitive to the enzyme–substrate complex. In all cases, the model is described by an addition parameter $K_I$.

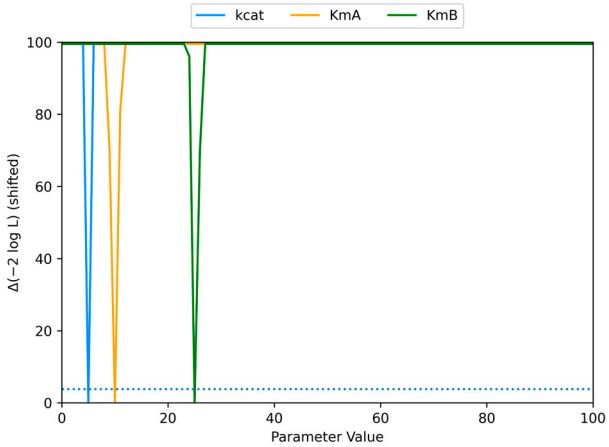


**Figure 1.** Likelihood profile of parameter estimation after 10th round for a reaction without inhibition. Blue line represents $k_{cat}$ in $s^{-1}$, orange line represents $K_{M,A}$ in mM, and green line represents $K_{M,B}$ in mM. The dashed line marks the threshold corresponding to the 95% confidence interval.

#### 3.2.1. Competitive Inhibition by Component B

In this example, component B induces a competitive inhibition of the free enzyme, which implies an ordered mechanism, as usual for a ping-pong mechanism, where A must bind first. The additional parameter describing the model is $K_{IC,B}$. An example of this type of reaction is given by Zhang et al. [36]. The reaction can be described by Equation (5).

$$-\frac{d[A]}{dt} = -\frac{d[B]}{dt} = \frac{[E]_{tot} k_{cat} [A][B]}{(K_{M,A}(1 + \frac{[B]}{K_{iC,B}})[B]) + (K_{M,B}[A]) + ([A][B])} \quad (5)$$

Table 4 shows the estimated parameters for this 4-parameter model with parameters $k_{cat}$, $K_{M,A}$, $K_{M,B}$ and $K_{IC,B}$. The estimate of $k_{cat}$ in round 1 differs from later rounds and is associated with a comparatively wide confidence interval, similar to the estimation of $k_{cat}$ from the previous model. From round 2 onward, $k_{cat}$ values are tightly clustered around 5 $s^{-1}$, with narrow and stable confidence intervals that remain unchanged through to round 10. For $K_{M,A}$, $K_{M,B}$, and $K_{IC,B}$, round 1 shows extremely wide confidence intervals spanning several orders of magnitude, indicating a bad estimation. In round 2, all three parameter estimates improve with substantially reduced confidence intervals. From round 3 onward, which is represented by six experiments, the estimates stabilise, and the confidence intervals become narrower. For this model, round 3 can be identified as a suitable stopping round, as from this round onward, the parameter estimates are very close to the true values and show only minor changes in the subsequent rounds. Similar to the previous case, the $R^2$ value is 0.98 in round 1, despite the wide confidence intervals and poor parameter estimates. From round 3 onwards, the $R^2$ indicates a very close fit to the data. As in case study 1, the nRMSE value decreases sharply between the first and second rounds and then continues to decrease in small steps with each subsequent round.

The profile likelihood plots of the four parameters shown in Figure 2 correspond to the last round. Similar to the 3-parameter model, all profiles show a single, sharp minimum located near the true parameter value. A steep increase is also visible on both sides of the minimum with very narrow confidence intervals. The profile likelihood plots from the earlier rounds show behaviour consistent with the trends reported in Table 4.

**Table 4.** Parameters estimated in various rounds for a reaction with a competitive inhibition by component B. Values in brackets represent the lower and upper limits of the 95% confidence interval.

| Round No. | $k_{cat}$ [$s^{-1}$] | $K_{M,A}$ [mM] | $K_{M,B}$ [mM] | $K_{IC,B}$ [mM] | $R^2$ [-] | nRMSE [-] |
|---|---|---|---|---|---|---|
| 1 | 1.34 [0.94, 1.91] | 2.17 [$7.77 \times 10^{-07}$, $6.08 \times 10^{6}$] | 0.001 [$1.93 \times 10^{-22}$, $5.19 \times 10^{21}$] | 1000.00 [$1.93 \times 10^{-22}$, $5.19 \times 10^{21}$] | 0.98 | 0.1780 |
| 3 | 5.00 [5.00, 5.01] | 10.36 [6.97, 15.39] | 24.95 [21.35, 29.16] | 61.96 [41.37, 92.79] | 1.00 | 0.0020 |
| 10 | 5.00 [5.00, 5.01] | 9.82 [8.98, 10.73] | 25.35 [24.65, 26.07] | 58.74 [53.53, 64.45] | 1.00 | 0.0015 |

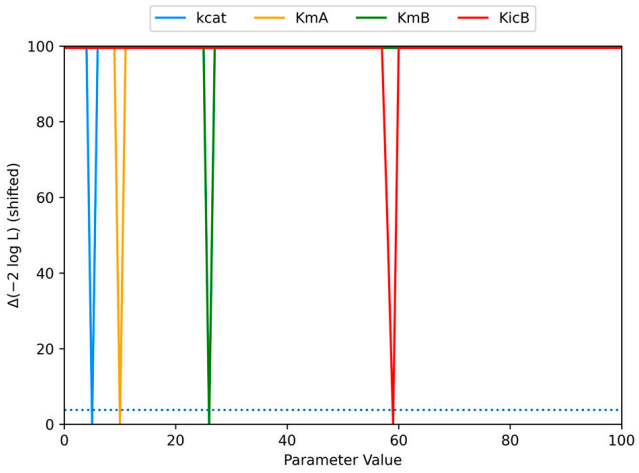


**Figure 2.** Likelihood profile of parameter estimation after 10th round for a reaction with a competitive inhibition by component B. Blue line represents $k_{cat}$ in $s^{-1}$, orange line represents $K_{M,A}$ in mM, green line represents $K_{M,B}$ in mM and red line represents $K_{IC,B}$ in mM. The dashed line marks the threshold corresponding to the 95% confidence interval.

### 3.2.2. Uncompetitive Inhibition by Component B

For the case of an uncompetitive inhibition by component B, it is assumed that B inhibits the enzyme–substrate complex before the first product is released and leaving the modified enzyme E*. Here the additional fourth parameter is $K_{IU,B}$. The reaction can be described by Equation (6).

$$-\frac{d[A]}{dt} = -\frac{d[B]}{dt} = \frac{[E]_{tot} k_{cat} [A][B]}{(K_{M,A}[B]) + (K_{M,B}[A]) + ([A][B](1 + \frac{[B]}{K_{iU,B}}))} \quad (6)$$

Table 5 reports the parameter estimates of the 4-parameter model with this uncompetitive inhibition by B. For $k_{cat}$, across all rounds, the value increases gradually around 2–2.7 $s^{-1}$ and remains well below the true value of 5 $s^{-1}$, despite consistently narrow confidence intervals from round 2 onward. These narrow confidence intervals suggest a good parameter estimation, which is not the case here, and the same can be said about the $R^2$ value. $K_{M,A}$ stays fixed at very small values with extremely wide confidence intervals in most rounds, showing only small deviations in rounds 6 and 7. A similar trend is evident for $K_{M,B}$, where its estimates are poor with very high confidence intervals until round 7, after which estimates with narrower confidence intervals are achieved; however, they remain far from the true value of 25 mM. $K_{IU,B}$ shows stable and narrow confidence intervals from round 2 onward; however, the estimates decrease from 230 mM to 140 mM, remaining substantially higher than the true value of 80 mM. Overall, none of the parameters converges to their true values for the given set of data, but only the confidence intervals of

$K_{M,A}$ suggest a bad estimation. The $R^2$ values increase from 0.98 in round 1 to 0.99 in later rounds. Notably, even in early rounds where the parameter estimates deviate strongly from the true values, $R^2$ is already high, indicating a close fit to the data despite poor parameter estimation. As described before, the nRMSE value decreases sharply between the first and second rounds. However, from the second round onward, the value fluctuates around 0.02, indicating no consequent improvement.

**Table 5.** Parameters estimated in various rounds for a reaction with an uncompetitive inhibition by component B. Values in brackets represent the lower and upper limits of the 95% confidence interval.

| Round No. | $k_{cat}$ [$s^{-1}$] | $K_{M,A}$ [mM] | $K_{M,B}$ [mM] | $K_{IU,B}$ [mM] | $R^2$ [-] | nRMSE [-] |
|---|---|---|---|---|---|---|
| 1 | 2.04 [0.44, 9.38] | 0.05 [$1.93 \times 10^{-22}$, $5.19 \times 10^{21}$] | 3.67 [0.015, 919.83] | 333.43 [$1.93 \times 10^{-22}$, $5.19 \times 10^{21}$] | 0.98 | 0.1754 |
| 5 | 2.67 [2.66, 2.67] | 0.006 [$1.93 \times 10^{-22}$, $5.26 \times 10^{18}$] | 0.001 [$1.93 \times 10^{-22}$, $5.19 \times 10^{21}$] | 146.04 [145.70, 146.37] | 0.99 | 0.0211 |
| 10 | 2.80 [2.79, 2.81] | 0.001 [$1.93 \times 10^{-22}$, $5.19 \times 10^{21}$] | 1.72 [1.46, 2.03] | 140.31 [140.00, 140.62] | 0.99 | 0.0180 |

The profile likelihood for this model with uncompetitive inhibition by B is presented in Figure 3 for round 10. Only $k_{cat}$ has a minimum near its true value of 5 $s^{-1}$. The minima of $K_{M,A}$ and $K_{M,B}$ are effectively at zero, while $K_{IU,B}$ is near 100 mM. The narrow confidence intervals imply a good estimation, even though the estimated values do not represent the true values at all ($K_{M,A} \approx 0$ mM vs. true 10 mM, $K_{M,B} \approx 2$ mM vs. true 25 mM, $K_{IU,B} \approx 100$ mM vs. true 80 mM). Since the display of profiles is limited to 100—which, on the other hand, covers the correct solution space—the value at the boundary is estimated when estimating the profile likelihood for $K_{IU,B}$.

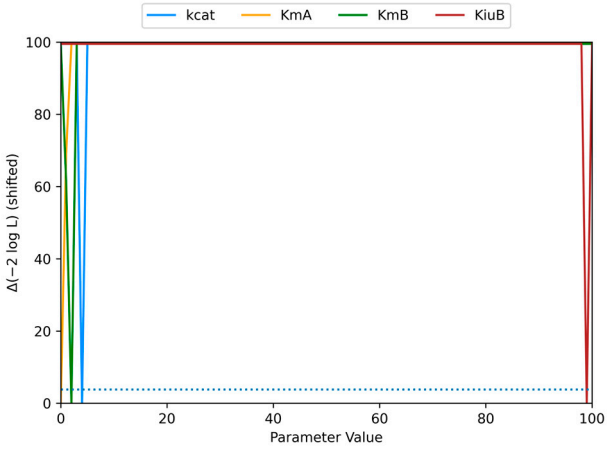


**Figure 3.** Likelihood profile of parameter estimation after 10th round for a reaction with an uncompetitive inhibition by component B. Blue line represents $k_{cat}$ in $s^{-1}$, orange line represents $K_{M,A}$ in mM, green line represents $K_{M,B}$ in mM and brown line represents $K_{IU,B}$ in mM. The dashed line marks the threshold corresponding to the 95% confidence interval.

### 3.2.3. Competitive Inhibition of Component A

In this case, a competitive inhibition of component A on the modified enzyme E* is assumed. The additional parameter is therefore $K_{IC,A}$. The reaction can be described by Equation (7).

$$-\frac{d[A]}{dt} = -\frac{d[B]}{dt} = \frac{[E]_{tot} k_{cat}[A][B]}{(K_{M,A}[B]) + (K_{M,B}(1 + \frac{[A]}{K_{iC,A}})[A]) + ([A][B])} \quad (7)$$

The parameter estimates are shown in Table 6 for all four parameters. In round 1, all parameters show very wide confidence intervals with parameter estimates far from their true values. From round 2 onward, $k_{cat}$ and $K_{M,A}$ converge to values very close to their true parameter values with narrow confidence intervals, which remain consistent through round 10. $K_{M,B}$ and $K_{IC,A}$ also attain better estimation from round 2, with confidence intervals narrowing across rounds. However, both $K_{M,B}$ and $K_{IC,A}$ stabilise at values below their true parameters, and also, the confidence intervals do not cover the true values. The $R^2$ values increase from 0.98 to 0.99 from round 1 to round 2 onward, remaining stable across the estimation process. After a clear decrease between the first rounds, the nRMSE value fluctuates from the second round onwards, thus indicating no improvement in model quality. Overall, $k_{cat}$ and $K_{M,A}$ are identified quite early correctly, while $K_{M,B}$ and $K_{IC,A}$ do not converge to their true values despite improved precision in later rounds, ending up in a mis-parameterisation.

**Table 6.** Parameters estimated in various rounds for a reaction with a competitive inhibition by component A. Values in brackets represent the lower and upper limits of the 95% confidence interval.

| Round No. | $k_{cat}$ [$s^{-1}$] | $K_{M,A}$ [mM] | $K_{M,B}$ [mM] | $K_{IC,A}$ [mM] | $R^2$ [-] | nRMSE [-] |
|---|---|---|---|---|---|---|
| 1 | 1.82 [0.52, 6.38] | 1.79 [$1.02 \times 10^{-6}$, $3.15 \times 10^{6}$] | 1.35 [$2.70 \times 10^{-8}$, $6.74 \times 10^{7}$] | 6.92 [$4.49 \times 10^{-12}$, $1.07 \times 10^{13}$] | 0.98 | 0.1699 |
| 2 | 5.02 [4.99, 5.04] | 10.08 [9.27, 10.97] | 19.03 [12.99, 27.88] | 37.52 [25.10, 56.08] | 0.99 | 0.0026 |
| 10 | 5.00 [5.00, 5.01] | 10.10 [9.63, 10.59] | 17.70 [16.57, 18.91] | 34.86 [32.56, 37.32] | 0.99 | 0.0043 |

Figure 4 presents the profile likelihoods for the four parameters $k_{cat}$, $K_{M,A}$, $K_{M,B}$ and $K_{IC,A}$ in the model with competitive inhibition by A. $k_{cat}$ exhibits a single, sharp minimum at its true value of 5 $s^{-1}$. $K_{M,A}$ reaches a minimum at 15 mM with very narrow confidence intervals; although slightly above the true value of 10 mM, the deviation is moderate. While the other two parameters, $K_{M,B}$ and $K_{IC,A}$, both attain their true values with very narrow confidence intervals, indicating precise and reliable parameter estimation.

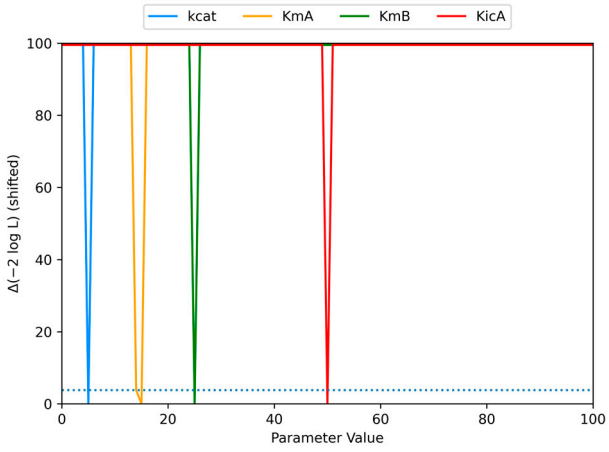


**Figure 4.** Likelihood profile of parameter estimation after 10th round for a reaction with a competitive inhibition by component A. Blue line represents $k_{cat}$ in $s^{-1}$, orange line represents $K_{M,A}$ in mM, green line represents $K_{M,B}$ in mM and red line represents $K_{IC,A}$ in mM. The dashed line marks the threshold corresponding to the 95% confidence interval.

#### 3.2.4. Uncompetitive Inhibition by Component A

Analogous to the uncompetitive inhibition by component B, this model also assumes an inhibition of the enzyme–substrate complex, before the first product is released. In this case, the inhibition is induced by component A, so the additional parameter is $K_{IU,A}$. The reaction can be described by Equation (8).

$$-\frac{d[A]}{dt} = -\frac{d[B]}{dt} = \frac{[E]_{tot} k_{cat} [A][B]}{(K_{M,A}[B]) + (K_{M,B}[A]) + ([A][B](1 + \frac{[A]}{K_{IU,A}}))} \quad (8)$$

The parameter estimates for the model with competitive inhibition by A show a clear progression across the 10 rounds (cf. Table 7). In the first four rounds, most parameters have narrow confidence intervals, but their estimates remain far from the true values. From round 5 onward, a sharp transition occurs, with estimates approaching the true values and maintaining narrow confidence intervals. While most parameters remain stable with the estimation in the subsequent rounds, $K_{M,B}$ shows a deviation in round 6, rising above its true value and ultimately stabilising around 31 mM in the final round, compared to the true value of 25 mM. Despite poor parameter estimates in the first round, $R^2$ is already high at 0.98. It increases slightly to 0.99 in subsequent rounds, and from round 5 onward, $R^2$ reaches 1.00. Like the confidence intervals, the nRMSE value shows a clear improvement between the fourth and fifth rounds. No further improvement is observed thereafter.

**Table 7.** Parameters estimated in various rounds for a reaction with an uncompetitive inhibition by component A. Values in brackets represent the lower and upper limits of the 95% confidence interval.

| Round No. | $k_{cat}$ [$s^{-1}$] | $K_{M,A}$ [mM] | $K_{M,B}$ [mM] | $K_{IU,A}$ [mM] | $R^2$ [-] | nRMSE [-] |
|---|---|---|---|---|---|---|
| 1 | 1.32 [0.93, 1.87] | 2.13 [$1.93 \times 10^{-22}$, $5.19 \times 10^{21}$] | 0.002 [$1.93 \times 10^{-22}$, $5.19 \times 10^{21}$] | 998.42 [$1.93 \times 10^{-22}$, $5.19 \times 10^{21}$] | 0.98 | 0.1775 |
| 4 | 2.30 [2.28, 2.31] | 0.002 [$1.93 \times 10^{-22}$, $5.19 \times 10^{21}$] | 1.35 [0.80, 2.28] | 150.44 [149.38, 151.51] | 0.99 | 0.0494 |
| 5 | 4.99 [4.97, 5.02] | 9.77 [8.92, 10.70] | 25.56 [23.86, 27.38] | 70.07 [69.79, 70.36] | 1.00 | 0.0018 |
| 10 | 4.99 [4.97, 5.00] | 9.69 [9.02, 10.41] | 31.24 [29.79, 32.75] | 70.21 [70.00, 70.42] | 1.00 | 0.0033 |

The likelihood profiles in Figure 5 are presented for round 10 for this 4-parameter model with uncompetitive inhibition by component A. The parameters $k_{cat}$, $K_{M,A}$ and $K_{IU,A}$ exhibit minima at their true values with extremely narrow confidence intervals. $K_{M,B}$ also has a minimum very close to its true value with narrow confidence intervals; however, an additional local minimum is observed near the true value, close to the likelihood threshold. This indicates the presence of a second minimum for this parameter, given the current data, but quite close to the true minimum.

### *3.3. Case Study 3: Two Inhibitions Described by Five Parameters*

This subchapter handles two exemplary cases with two inhibitions. They represent a mixture of the candidates from the second case study, where the parameters were identified correctly or incorrectly, with a wide confidence interval indicating a non-identifiability or even with narrow intervals, ending up in a mis-parameterisation. Other model candidates with five parameters are available in our repository, but they will not be discussed in this section.

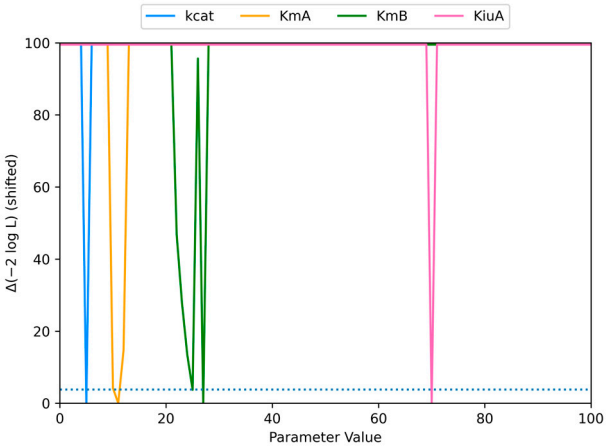


**Figure 5.** Likelihood profile of parameter estimation after 10th round for a reaction with an uncompetitive inhibition by component A. Blue line represents $k_{cat}$ in $s^{-1}$, orange line represents $K_{M,A}$ in mM, green line represents $K_{M,B}$ in mM and pink line represents $K_{IU,A}$ in mM. The dashed line marks the threshold corresponding to the 95% confidence interval.

#### 3.3.1. Competitive Inhibition by Components A and B

For this 5-parameter model, it is assumed that the enzyme is subject to competitive inhibition by components A and B. Here, component A is competitive to the modified enzyme E*, while B is competitive for the enzyme E if the mechanism is ordered and component A must bind first. This setup introduces two additional parameters: $K_{IC,A}$ and $K_{IC,B}$. An example was reported by Stromme and Theodorsen [37] and Waghmare et al. [32]. The reaction can be described by Equation (9).

$$-\frac{d[A]}{dt} = -\frac{d[B]}{dt} = \frac{[E]_{tot} k_{cat} [A][B]}{(K_{M,A}(1 + \frac{[B]}{K_{iC,B}})[B]) + (K_{M,B}(1 + \frac{[A]}{K_{iC,A}})[A]) + ([A][B])} \quad (9)$$

The parameter estimates in Table 8 show rapid convergence across the 10 rounds. $k_{cat}$ stabilises very close to its true value from round 2 onward with very narrow confidence intervals. $K_{M,A}$ and $K_{M,B}$ approach their true values in round 3 onward with slightly wide confidence intervals. $K_{IC,A}$ converges near its true value of 50 mM, and $K_{IC,B}$ stabilises around 65 mM, slightly over-estimating its true value of 60 mM. Overall, by round 10, all parameters have achieved estimates close to their expected values with reasonably narrow confidence intervals, covering all true values. Also, for this complex model, the $R^2$ value after the first round is 0.98, indicating a good fit, even if the estimated parameters are far away from the true values. The $R^2$ value already increases to 1.00 from round 3 onward. In this scenario as well, the nRMSE value only shows a clear decrease after the first round and fluctuates afterwards, indicating that further model accuracy is not represented.

**Table 8.** Parameters estimated in various rounds for a reaction with a competitive inhibition by component A and a competitive inhibition by component B. Values in brackets represent the lower and upper limits of the 95% confidence interval.

| Round No. | $k_{cat}$ [$s^{-1}$] | $K_{M,A}$ [mM] | $K_{M,B}$ [mM] | $K_{IC,A}$ [mM] | $K_{IC,B}$ [mM] | $R^2$ [-] | nRMSE [-] |
|---|---|---|---|---|---|---|---|
| 1 | 1.70 [0.54, 5.37] | 1.36 [$1.93 \times 10^{-22}$, $5.19 \times 10^{21}$] | 0.58 [$1.93 \times 10^{-22}$, $5.19 \times 10^{21}$] | 2.75 [$1.93 \times 10^{-22}$, $5.19 \times 10^{21}$] | 4.73 [$1.93 \times 10^{-22}$, $5.19 \times 10^{21}$] | 0.98 | 0.1702 |
| 3 | 5.00 [4.98, 5.02] | 10.39 [7.33, 14.72] | 24.50 [20.87, 28.76] | 48.93 [41.55, 57.63] | 62.33 [42.94, 90.47] | 1.00 | 0.0018 |
| 10 | 5.00 [4.99, 5.01] | 10.87 [8.59, 13.76] | 24.08 [21.59, 26.85] | 48.06 [43.00, 53.72] | 65.62 [51.39, 83.78] | 1.00 | 0.0022 |

In Figure 6, the likelihood profiles of this 5-parameter model after the 10th round are shown. All parameters reach minima very close to their true value with extremely narrow confidence intervals—except for $K_{IC,B}$, which slightly overestimates the true value of 60 mM—consistent with the parameter estimation derived from the Jacobian matrix approach. Despite this, each parameter displays a well-defined, single minimum, indicating reliable identifiability and reasonable convergence across the model, and meet their respective true parameter values.

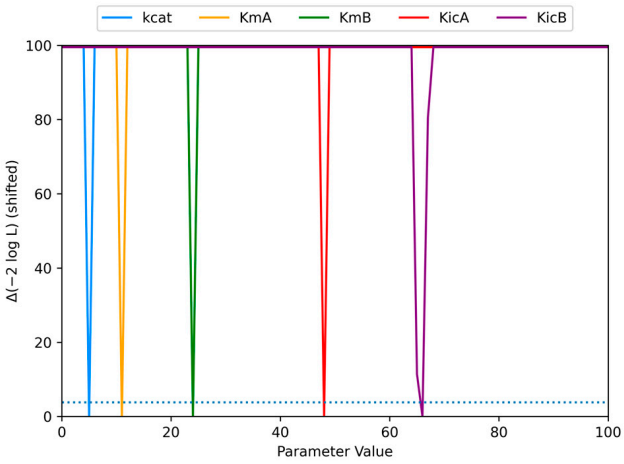


**Figure 6.** Likelihood profile of parameter estimation after 10th round for a reaction with a competitive inhibition by component A and a competitive inhibition by component B. Blue line represents $k_{cat}$ in $s^{-1}$, orange line represents $K_{M,A}$ in mM, green line represents $K_{M,B}$ in mM, red line represents $K_{IC,A}$ in mM and purple line represents $K_{IC,B}$. The dashed line marks the threshold corresponding to the 95% confidence interval.

### 3.3.2. Competitive Inhibition by Component A and Uncompetitive Inhibition by Component B

In the model with competitive inhibition by A and uncompetitive inhibition by B, A is assumed to inhibit the modified enzyme E*, while B inhibits the enzyme–substrate complex. The additional parameters are $K_{IC,A}$ and $K_{IU,B}$, representing the respective inhibition constants. An example of competitive and uncompetitive substrate inhibition for a ping-pong mechanism is given by Picott et al. [38]. The reaction can be described by Equation (10).

$$-\frac{d[A]}{dt} = -\frac{d[B]}{dt} = \frac{[E]_{tot} k_{cat} [A][B]}{(K_{M,A}[B]) + (K_{M,B}(1 + \frac{[A]}{K_{iC,A}})[A]) + ([A][B](1 + \frac{[B]}{K_{iU,B}}))} \quad (10)$$

The parameter estimates across different estimation rounds in Table 9 show that $k_{cat}$ converges near its true value around 3 $s^{-1}$ from round 2 but shows no further improvement. In general, there is no improvement in the estimated values from round 3 onward. $K_{M,A}$ is close to zero, and therefore, misses the true value. $K_{M,B}$ converges at a value of 10 mM, which is below the true value. $K_{IC,A}$ stabilises around 42 mM from round 3 onward, below its true value, while $K_{IU,B}$ consistently converges near 128 mM, failing to reach its true value. The $R^2$ values are 0.98 in round 1 and then slightly increase to 0.99 from round 3 onward, showing a good fit to the data despite the parameter estimates not reaching their true values. In all cases, the confidence intervals also indicate a good estimation, but as the estimated parameters do not reflect the true values, this case study demonstrates a mis-parameterisation. Here as well, the nRMSE value only shows a clear decrease after the first round and fluctuates afterwards, so that further model accuracy is not represented.

**Table 9.** Parameters estimated in various rounds for a reaction with a competitive inhibition by component A and an uncompetitive inhibition by component B. Values in brackets represent the lower and upper limits of the 95% confidence interval.

| Round No. | $k_{cat}$ [$s^{-1}$] | $K_{M,A}$ [mM] | $K_{M,B}$ [mM] | $K_{IC,A}$ [mM] | $K_{IU,B}$ [mM] | $R^2$ [-] | nRMSE [-] |
|---|---|---|---|---|---|---|---|
| 1 | 1.71 [0.53, 5.50] | 2.20 [$1.93 \times 10^{-22}$, $5.19 \times 10^{21}$] | 0.58 [$1.93 \times 10^{-22}$, $5.19 \times 10^{21}$] | 2.84 [$1.93 \times 10^{-22}$, $5.19 \times 10^{21}$] | 64.07 [$1.93 \times 10^{-22}$, $5.19 \times 10^{21}$] | 0.98 | 0.1698 |
| 3 | 3.09 [3.09, 3.09] | 0.37 [0.01, 16.08] | 10.87 [8.26, 14.31] | 41.97 [31.69, 55.58] | 128.64 [128.50, 128.78] | 0.99 | 0.0181 |
| 10 | 3.09 [3.08, 3.10] | 0.37 [0.048, 2.94] | 10.87 [9.72, 12.17] | 41.97 [37.38, 47.12] | 128.64 [128.26, 129.02] | 0.99 | 0.0205 |

Figure 7 shows the profile likelihood plots of this 5-parameter model for the final round. Parameters $K_{M,A}$ and $K_{M,B}$ exhibit single, sharp minima with extremely narrow confidence intervals; however, the values are very close to zero. $K_{IU,B}$ also shows a sharp, single minimum, but it is offset from its true value of 80 mM. For $K_{IC,A}$, three distinct minima are visible, with the lowest touching the threshold at a value around 30 mM, considerably below its true value of 50 mM. The remaining two minima, however, do not touch the threshold, which indicates the presence of multiple local minima in the likelihood landscape for this dataset, not to be considered results of a reliable estimation. Only the parameter $k_{cat}$ is estimated correctly. Although the confidence intervals for all values indicate good identifiability, only some of the estimated value of $k_{cat}$ is close to the true values. In contrast, some parameters show clear mis-parameterisation.

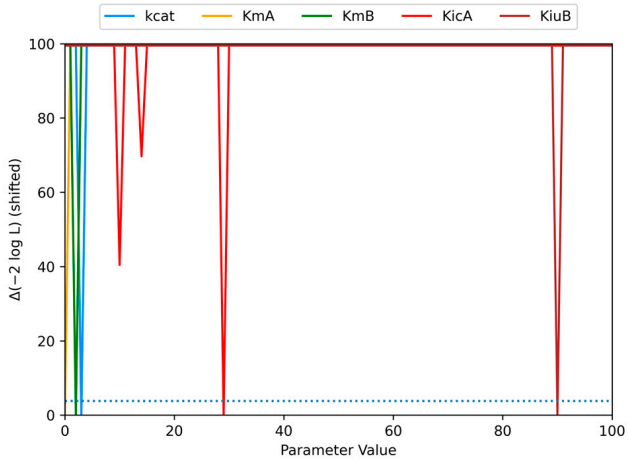


**Figure 7.** Likelihood profile of parameter estimation after 10th round for a reaction with a competitive inhibition by component A and an uncompetitive inhibition by component B. Blue line represents $k_{cat}$ in $s^{-1}$, orange line represents $K_{M,A}$ in mM, green line represents $K_{M,B}$ in mM, red line represents $K_{IC,A}$ in mM and brown line represents $K_{IU,B}$. The dashed line marks the threshold corresponding to the 95% confidence interval.

### *3.4. Case Study 4: Three Inhibitions Described by Six Parameters*

In this case study, only one candidate is investigated in detail, with a total of three inhibitions by components A and B being assumed. For this model, competitive inhibition by A and both competitive and uncompetitive inhibition by B are assumed. The reaction can be described by Equation (11).

$$-\frac{d[A]}{dt} = -\frac{d[B]}{dt} = \frac{[E]_{tot} k_{cat}[A][B]}{(K_{M,A}(1+\frac{[B]}{K_{iC,B}})[B]) + (K_{M,B}(1+\frac{[A]}{K_{iC,A}})[A]) + ([A][B](1+\frac{[B]}{K_{iU,B}}))} \quad (11)$$

Here, the component A inhibits the modified enzyme E*, while component B inhibits the free enzyme (competitive), and also inhibits the enzyme–substrate complex (uncompetitive). The additional parameters in this model are $K_{IC,A}$, $K_{IC,B}$, and $K_{IU,B}$. The parameter estimates across different rounds in Table 10 show that $k_{cat}$ remains stable around 3.3 $s^{-1}$ from round 2 onward; however, it stays below its true value. While $K_{M,B}$ stabilises near 2.4 mM with moderate confidence intervals, $K_{M,A}$ stays very low throughout the rounds with wide confidence intervals, indicating high uncertainty. $K_{IC,B}$ stabilises around 15 mM, considerably below its true value, with wide confident intervals, and $K_{IU,B}$ consistently converges near 119 mM, also above its true value. $K_{IC,A}$ shows little variation for all 10 rounds, remaining around 21 mM as compared to its true value of 50 mM, with relatively narrow confidence intervals. Apart from a reduction in the confidence intervals, the estimated parameters remain constant from the second round onwards. The confidence intervals are wider than in the case studies before, but still imply a good parameterisation, despite being an incorrect one. $R^2$ remains high, ranging from 0.98 to 0.99 across all rounds, despite the parameter estimates not converging to their true values across the 10 rounds. As before, the nRMSE value only shows a clear decrease after the first round. The fluctuation afterwards shows no further improvement in the model accuracy.

**Table 10.** Parameters estimated in various rounds for a reaction with a competitive inhibition by component A and a competitive as well as an uncompetitive inhibition by component B. Values in brackets represent the lower and upper limits of the 95% confidence interval.

| Round No. | $k_{cat}$ [$s^{-1}$] | $K_{M,A}$ [mM] | $K_{M,B}$ [mM] | $K_{IC,B}$ [mM] | $K_{IU,B}$ [mM] | $K_{IC,A}$ [mM] | $R^2$ [-] | nRMSE [-] |
|---|---|---|---|---|---|---|---|---|
| 1 | 1.76 [0.47, 6.63] | 0.75 [$1.93 \times 10^{-22}$, $5.19 \times 10^{21}$] | 2.32 [$1.93 \times 10^{-22}$, $5.19 \times 10^{21}$] | 15.37 [$1.93 \times 10^{-22}$, $5.19 \times 10^{21}$] | 115.45 [$1.93 \times 10^{-22}$, $5.19 \times 10^{21}$] | 21.32 [$1.93 \times 10^{-22}$, $5.19 \times 10^{21}$] | 0.98 | 0.1690 |
| 2 | 3.30 [3.29, 3.32] | 0.70 [$1.50 \times 10^{-6}$, $3.25 \times 10^{5}$] | 2.45 [0.62, 9.69] | 15.70 [$3.00 \times 10^{-5}$, $8.20 \times 10^{6}$] | 119.75 [118.62, 120.89] | 21.28 [4.15, 109.06] | 0.99 | 0.0295 |
| 10 | 3.30 [3.28, 3.33] | 0.70 [0.14, 3.42] | 2.45 [1.55, 3.86] | 15.70 [3.14, 78.40] | 119.75 [118.91, 120.60] | 21.28 [13.42, 33.75] | 0.99 | 0.0342 |

Figure 8 shows the profile likelihoods for this 6-parameter model. Parameters $k_{cat}$ and $K_{IU,B}$ exhibit sharp, well-defined minima close to their true values, with extremely narrow confidence intervals. $K_{M,A}$, $K_{M,B}$, and $K_{IC,A}$ each display a single sharp minimum. However, $K_{M,B}$ and $K_{IC,A}$ converge to values substantially different from their true parameters, while $K_{M,A}$ converges very close to zero, with all showing very narrow confidence intervals. For $K_{IC,B}$, three distinct minima are observed, all reaching the confidence threshold, with the lowest minimum around 5 mM, far below the true value of 60 mM, indicating the presence of multiple minima. Overall, while two parameters are well-estimated, others remain ambiguous due to the complex likelihood landscape for the given dataset.

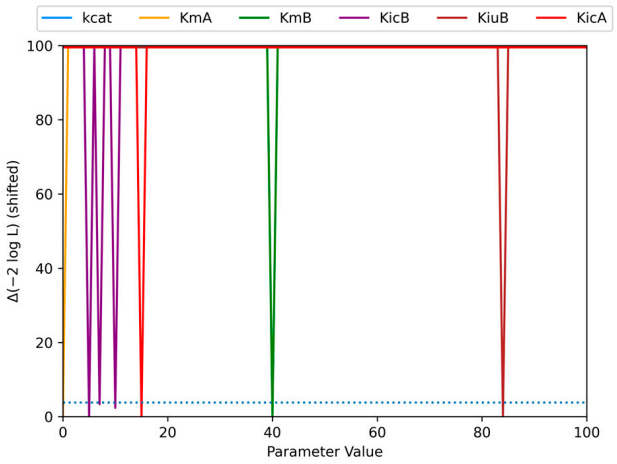


**Figure 8.** Likelihood profile of parameter estimation after 10th round for a reaction with a competitive inhibition by component A and a competitive and an uncompetitive inhibition by component B. Blue line represents $k_{cat}$ in $s^{-1}$, orange line represents $K_{M,A}$ in mM, green line represents $K_{M,B}$ in mM, purple line represents $K_{IC,B}$ in mM, brown line represents $K_{IU,B}$ and red line represents $K_{IC,A}$. The dashed line marks the threshold corresponding to the 95% confidence interval.

### *3.5. Case Study 5: Four Inhibitions Described by Seven Parameters*

For this final case study, both substrates are assumed to exert competitive inhibition on the enzyme or modified enzyme, represented by $K_{IC,B}$ and $K_{IC,A}$, and uncompetitive inhibition on the enzyme–substrate complex before product release, represented by $K_{IU,A}$ and $K_{IU,B}$, resulting in a total of seven parameters. The reaction can be described by Equation (12).

$$-\frac{d[A]}{dt} = -\frac{d[B]}{dt} = \frac{[E]_{tot} k_{cat} [A][B]}{(K_{M,A}(1+\frac{[B]}{K_{iC,B}})[B]) + (K_{M,B}(1+\frac{[A]}{K_{iC,A}})[A]) + ([A][B](1+\frac{[B]}{K_{iU,B}})(1+\frac{[A]}{K_{iU,A}}))} \quad (12)$$

Table 11 presents the parameter estimates for this 7-parameter model. In rounds 1 through 4, most parameters exhibit extremely wide confidence intervals, often spanning many orders of magnitude, reflecting high uncertainty, and the estimates deviate substantially from the true values. From round 5 onward, $k_{cat}$ stabilises with very narrow confidence intervals while the other parameters remain far from their true values. A sharp transition occurs in round 10, where all parameters attain estimates close to the true values; however, confidence intervals remain wide for most parameters except $K_{IU,B}$ and $K_{IU,A}$. $R^2$ values remain high throughout the estimation process in the range of 0.98 to 0.99, despite most parameters not reaching their true values until the final round, where $R^2$ shows the correct representation of the estimated parameters. Overall, early rounds exhibit high uncertainty and instability, mid rounds show partial stabilisation for some parameters, and full convergence of all seven parameters is achieved only by round 10. Interestingly, the nRMSE shows a slight increase between rounds 2 and 4, followed by a consistent decrease, which suggests a better model estimate.

**Table 11.** Parameters estimated in various rounds for a reaction with a competitive inhibition by component A as well as B, and an uncompetitive inhibition by component A as well as B. Values in brackets represent the lower and upper limits of the 95% confidence interval.

| Round No. | $k_{cat}$ [$s^{-1}$] | $K_{M,A}$ [mM] | $K_{M,B}$ [mM] | $K_{IC,A}$ [mM] | $K_{IC,B}$ [mM] | $K_{IU,B}$ [mM] | $K_{IU,A}$ [mM] | $R^2$ [-] | nRMSE [-] |
|---|---|---|---|---|---|---|---|---|---|
| 1 | 199.99 [$1.93 \times 10^{-22}$, $5.19 \times 10^{21}$] | 34.34 [$1.93 \times 10^{-22}$, $5.19 \times 10^{21}$] | 467.11 [$1.93 \times 10^{-22}$, $5.19 \times 10^{21}$] | 5.41 [$1.93 \times 10^{-22}$, $5.19 \times 10^{21}$] | 1000.00 [$1.93 \times 10^{-22}$, $5.19 \times 10^{21}$] | 1000.00 [$1.93 \times 10^{-22}$, $5.19 \times 10^{21}$] | 1000.00 [$1.93 \times 10^{-22}$, $5.19 \times 10^{21}$] | 0.98 | 0.1693 |
| 5 | 4.62 [4.60, 4.63] | 0.001 [$1.93 \times 10^{-22}$, $5.19 \times 10^{21}$] | 2.90 [0.73, 11.60] | 0.97 [0.24, 3.95] | 1000.00 [$1.93 \times 10^{-22}$, $5.19 \times 10^{21}$] | 39.87 [39.32, 40.43] | 217.64 [211.98, 223.44] | 0.99 | 0.0138 |
| 10 | 4.98 [4.88, 5.08] | 10.16 [5.89, 17.52] | 25.32 [20.08, 31.92] | 50.85 [38.43, 67.29] | 62.73 [34.60, 113.73] | 79.97 [78.59, 81.38] | 70.39 [69.18, 71.63] | 0.99 | 0.0015 |

The likelihood profiles for this 7-parameter model are shown in Figure 9. Similar to the 6-parameter model, $k_{cat}$, $K_{IU,B}$ and $K_{IU,A}$ show sharp, single minima with steep rise on both sides of the minimum. $K_{M,A}$ (a) and $K_{IC,B}$ (b) exhibit highly oscillatory profiles with multiple local minima, similar to the previous model. $K_{M,B}$ shows three minima in this model, with the lowest minimum corresponding to the true parameter and narrower confidence intervals. The newly introduced parameter, $K_{IC,A}$, displays two minima, with the lower minimum near the true value and slightly wider confidence intervals.

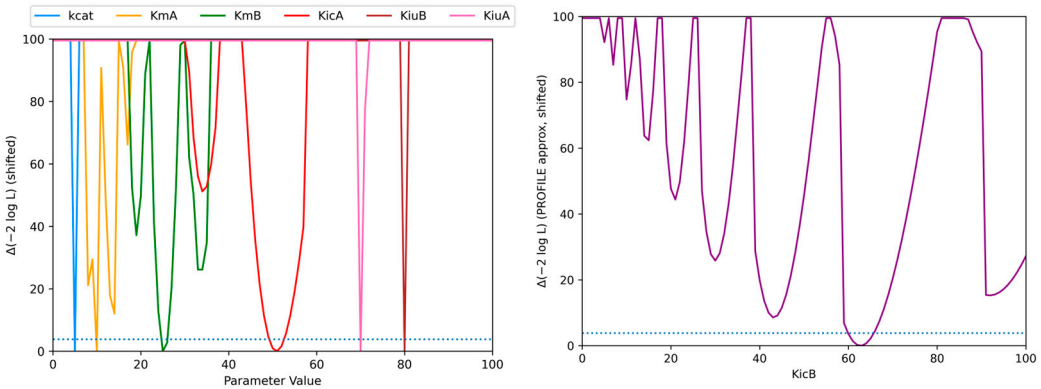


(**a**) (**b**)

**Figure 9.** Likelihood profile of parameter estimation after 10th round for a reaction with a competitive inhibition by component A as well as B and an uncompetitive inhibition by component A as well as B. (**a**) Blue line represents $k_{cat}$ in $s^{-1}$, orange line represents $K_{M,A}$ in mM, green line represents $K_{M,B}$ in mM, red line represents $K_{IC,A}$ in mM, brown line represents $K_{IU,B}$, and pink line represents $K_{IU,A}$ and (**b**) violet line $K_{IC,B}$. The dashed line marks the threshold corresponding to the 95% confidence interval.

## 4. Discussion

Previous work has shown that the tQSSA approach presented here enables clear identification of the kinetic parameters of a simple single-substrate reaction with two parameters [27]. However, there have been no reports in the literature to date on the extent to which this approach can also be applied to more complex models. In our repository, we provide 16 candidates of a ping-pong mechanism with various combinations of substrate inhibitions that occur. However, in this chapter, we use the same structure as in Section 3 and discuss the different case studies presented in the results.

First, the overall result of the coefficient of determination and the normalised root mean square error is examined: In all cases, some parameters were far from their true values despite a good fit. This happens because $R^2$ only measures how well the model reproduces the observed data, not whether the individual parameter values are correct. Multiple

combinations of parameter sets can produce very similar estimation results, especially in complex models, leading to high $R^2$ even when the parameters are inaccurate. Therefore, $R^2$ alone cannot guarantee correct parameter identification and should be considered alongside confidence intervals and parameter trends in the estimation process. The nRMSE scores somewhat better. In all case studies, it consistently shows an improvement in the value from the second round onward. However, the results vary considerably between the individual case studies thereafter. Particularly with complex models, the nRMSE also fails to demonstrate a consistent improvement in parameter estimation.

### *4.1. Discussion for Case Study 1*

For the application of a 3-parameter model equation, all kinetic parameters could be identified very early on and without ambiguity. After the first round, which corresponds to two experiments, the values were estimated incorrectly, but this was evident from the large confidence intervals. After just the second round, which corresponds to the performance of four experiments in total, the parameters were correctly identified, and the accuracy in the form of confidence intervals is also acceptable. This applies both to the calculation of parameters and confidence intervals using the classic method via the Jacobi matrix and to the more complex representation via likelihood profiles. Thus, as a first step, it was successfully demonstrated that the method of parameter estimation via the total quasi-steady-state assumption (tQSSA) is possible and leads to correct results beyond simple 2-parameter models, and over-parameterisation does not occur here.

### *4.2. Discussion for Case Study 2*

Case study 2 dealt with four different examples. In each case, inhibition caused by one specific substrate component occurred. The inhibition was either competitive or non-competitive. The results reveal initial inconsistencies: the kinetic parameters of competitive inhibition by B were correctly identified in this study and covered approximately accurately by the confidence intervals. However, the kinetic parameters of uncompetitive inhibition by B could not be correctly identified. When the confidence intervals were calculated via the Jacobian matrix, only the confidence interval for one parameter indicated that identification was not possible. Normally, this would be interpreted to mean that this parameter—especially since the value was estimated to be 0.001 mM—is not present and therefore the assumed reaction mechanism would be incorrect. However, this is not the case in this example. If the method of likelihood profiles was used, only the $k_{cat}$ parameter was estimated correctly, while in all cases, the profile indicated a good estimation for all parameters, but did not match the true parameters. This shows for the first time that the tQSSA assumption may not be able to correctly estimate a 4-parameter model under the given circumstances.

If uncompetitive inhibition by component A is assumed, the underlying parameter values were, in general, correctly estimated in the example shown here and also very well identified within the confidence intervals. For the Jacobian method, only one parameter was overestimated, but within an acceptable error, while the profile likelihood results in a correct estimation of all values. Remarkably, the model equation is extended in the same way for the individual uncompetitive inhibitions. In the denominator, the term ([A][B]) is extended by $(1 + [A]/K_{IU,A})$ or $(1 + [A]/K_{IU,B})$, respectively. It can thus be seen that the estimation algorithm was able to estimate the values correctly in one example but was unable to do so in another. Even with the effort of 10 rounds (corresponding to 20 experiments), no correct identification could be achieved for the uncompetitive inhibition caused by component B. Thus, the interaction of the randomly selected kinetic parameter values, as well as the selected initial concentrations for the first round of experiments, has

a decisive influence on identifiability. However, it should be noted that the unsuccessful estimation of $K_{IU,B}$ is indicated by the wide confidence intervals for $K_{M,A}$, which is only the case with the Jacobian matrix method. So, mis-parameterisation can occur.

The correct estimation in the case of competitive inhibition by A also shows weaknesses. Two parameters could be correctly identified, and the confidence intervals also show clear identification. However, using the Jacobian matrix method, two parameters were incorrectly estimated and were not covered by the confidence intervals. Nevertheless, the incorrectly estimated values are still within the same order of magnitude as the true parameter values, so this misestimation can be considered acceptable. In contrast, the likelihood profile method shows a significantly better estimate. All four parameters were correctly identified, which demonstrates an advantage of this more complex method.

### *4.3. Discussion for Case Study 3*

Also, for the application of the tQSSA approach for a 5-parametric model, the results are inconsistent. For the example of two competitive inhibitions, the identification of all parameters was successful, and all true parameters were met within the confidence intervals of each parameter. However, if a competitive inhibition by component A and an uncompetitive inhibition by component B is assumed, the algorithm fails in identifying the correct parameters, even though the confidence intervals suggested a correct identification.

Even when considering the other model candidates (data can be generated via the repository), there is no consistent trend. It is neither the case that certain $K_I$ values are always estimated correctly, nor are certain $K_I$ values always estimated poorly. Thus, in the case of this study, no consistent statement can be made for model depths of five parameters or more. However, under certain circumstances, a correct identification is possible.

### *4.4. Discussion for Case Study 4*

In the 6-parameter model presented in this study, the parameters underlying the model could not be estimated correctly, although the confidence intervals suggest good identifiability. However, a comparison of this example with other 6-parameter models (cf. repository) shows that six parameters are not the limit. In this study, for example, all six parameters could be well identified within an acceptable tolerance range in a model with competitive and uncompetitive inhibition by component A and uncompetitive inhibition by component B. This shows that six parameters are not the limit of over-parameterisation when using the tQSSA approach. However, this is not a generally valid statement, as in a broader comparison of all candidates with six parameters, no $K_I$ value stands out in either direction.

### *4.5. Discussion for Case Study 5*

The last example considered a model with a total of four inhibitions and thus seven parameters in total. Although in the previous case studies with fewer parameters, the parameters were not correctly identified in some models, in this example, all parameters could be correctly identified. This shows that the tQSSA approach can be applied to very complex models and is capable of correctly estimating the intrinsic parameters of an enzyme. In this particular case, over-parameterisation was not visible.

### *4.6. General Aspects to Improve Parameter Estimation*

The aim of this study was to generally examine whether the tQSSA approach can also be applied to enzymatic kinetics for the successful estimation of kinetic parameters when more than two parameters are present. This was successfully demonstrated for a three-parameter model. Another aspect was the question of whether this approach could also be used to counteract the over-parameterisation mentioned in the literature. In principle,

the approach was also able to correctly identify parameters when four or more parameters were present. However, this is also the range in which the first mis-parameterisation occurs. This shows that the tQSSA approach certainly has the potential to correctly identify the parameter values of highly parameterised models; however, there is no guarantee of this. The approach, therefore, needs to be improved in future work.

It should be noted that the focus here was on feasibility. It is well known that the number of data points per experiment also has an influence on the success of the estimation. Similarly, there are different sections in progress curves with significant substrate depletion: initially, the concentration curve is almost linear; in the middle, there is a curved area; towards the end, there are hardly any changes in the concentration. It should be noted here that the highest information density is in the curved area [39]. Therefore, the best time to take a sample can also be implemented into the decision [40]. The mathematical method of integration used also has an influence on the result, as do the starting values of the estimation [13]. Based on these topics, the parameter estimation can still be adjusted to improve the estimation method.

## 5. Conclusions and Outlook

In this study, the total quasi-steady-state assumption (tQSSA) approach was successfully applied for the first time to identify parameters in kinetic models with more than two parameters by progress curve analysis. Model-based optimised experimental design was used for this purpose. The questions of when the tQSSA approach fails and when over-parameterisation in the form of non-identifiability of the parameters occurs were also investigated. To this end, the complexity of the kinetics was increased step by step and the number of parameters was increased from 3 to 7. In silico studies were used because this is the only way to specify the intrinsic characteristics of an enzyme through kinetic parameters. In order to cover a real case, the experimental data on which the estimation is based were noisy. Overall, the picture is very mixed: in one case, the model parameters could not be correctly identified with only four parameters. In another case, however, up to seven parameters could be correctly identified. Possibilities for improving parameter estimation in general were also discussed, which would enable correct identification even for models that cannot be correctly identified in this study.

This shows that the tQSSA approach offers a very good opportunity to meet the challenge of over-parameterisation. At present, however, there are still limitations that need to be addressed in future research. In particular, optimal experimental design strategies could be extended to jointly optimise sampling times, initial concentrations, and experimental conditions based on sensitivity or Fisher information analyses in order to maximise parameter identifiability. Such approaches would allow a more systematic extraction of information from experimental data.

**Supplementary Materials:** The following supporting information can be downloaded at: https://www.mdpi.com/article/10.3390/appliedchem6020025/s1, Figure S1: Time course data of a reaction without inhibition; Figure S2: Time course data of a reaction with competitive inhibition by component B; Figure S3: Time course data of a reaction with uncompetitive inhibition by component B; Figure S4: Time course data of a reaction with competitive inhibition by component A; Figure S5: Time course data of a reaction with uncompetitive inhibition by component A; Figure S6: Time course data of a reaction with competitive inhibition by components A and B; Figure S7: Time course data of a reaction with competitive inhibition by component A and uncompetitive inhibition by component B; Figure S8: Time course data of a reaction with competitive inhibition by component A and competitive and uncompetitive inhibition by component B; Figure S9: Time course data of a reaction with competitive and uncompetitive inhibition by component A and competitive and uncompetitive inhibition by component B.

**Author Contributions:** Conceptualization, T.W. and P.N.; Methodology, T.W. and P.N.; Investigation, T.W. and P.N.; Writing—original draft preparation, T.W. and P.N.; Writing—review and editing, T.W. and P.N.; Visualisation, T.W. and P.N. All authors have read and agreed to the published version of the manuscript.

**Funding:** This research received no external funding.

**Institutional Review Board Statement:** Not applicable.

**Informed Consent Statement:** Not applicable.

**Data Availability Statement:** All codes and all data used is available under https://collaborating.tuhh.de/v-4/psi-public/tools4progresscurveanalysis.

**Acknowledgments:** During the preparation of this study, the authors used ChatGPT 5.2 Thinking for the purposes of code developing. The authors have reviewed and edited the output and take full responsibility for the content of this publication.

**Conflicts of Interest:** The authors declare no conflicts of interest.

## Abbreviations

The following abbreviations are used in this manuscript:

| | |
|---|---|
| FAIR | Findable, Accessible, Interoperable, Reusable |
| $k_{cat}$ | Turnover number |
| $K_M$ | Michaelis–Menten constant, with subscript for the respective substrate |
| $K_{IC}$ | Inhibition constant (for a corresponding substrate) for competitive inhibition |
| $K_{IU}$ | Inhibition constant (for a corresponding substrate) for uncompetitive inhibition |
| MAP | Maximum a posteriori |
| SE | Standard error |
| sQSSA | Standard quasi-steady-state approach |
| SSE | Sum of squared error |
| tQSSA | Total quasi-steady-state approach |
| σ | Standard deviation |
| Φ | Nuisance parameter of profile likelihood |
| $X^2_{1,0.95}$ | Chi-square for a level of significance of 0.05 |
| [A] | Concentration of substrate A, with subscript 0: initial concentration; with subscript obs: observed concentration; with subscript pred: predicted concentration |
| [B] | Concentration of substrate B, with subscript 0: initial concentration; with subscript obs: observed concentration; with subscript pred: predicted concentration |
| [E] | Concentration of enzyme, with subscript tot: total enzyme concentration |

## References

1. Erickson, B.; Nelson, J.E.; Winters, P. Perspective on opportunities in industrial biotechnology in renewable chemicals. *Biotechnol. J.* **2012**, *7*, 176–185. [CrossRef]
2. Gavrilescu, M.; Chisti, Y. Biotechnology-a sustainable alternative for chemical industry. *Biotechnol. Adv.* **2005**, *23*, 471–499. [CrossRef]
3. Boodhoo, K.; Flickinger, M.C.; Woodley, J.M.; Emanuelsson, E. Bioprocess intensification: A route to efficient and sustainable biocatalytic transformations for the future. *Chem. Eng. Process.-Process Intensif.* **2022**, *172*, 108793. [CrossRef]
4. Woodley, J.M. Bioprocess intensification for the effective production of chemical products. *Comput. Chem. Eng.* **2017**, *105*, 297–307. [CrossRef]
5. Woodley, J.M. Accelerating the implementation of biocatalysis in industry. *Appl. Microbiol. Biotechnol.* **2019**, *103*, 4733–4739. [CrossRef] [PubMed]
6. Gherdaoui, D.; Bouazza, F.; Ihadadene, S.; Yahoum, M.M.; Lefnaoui, S.; Amrane, A.; Mouni, L. Kinetic Modeling, Comparative Investigations, and a New Approach to Quantifying the Global Extraction Yield of Algerian Pomegranate Peel Phenolic Compounds. *AppliedChem* **2025**, *5*, 11. [CrossRef]

7. Johannsen, J.; Meyer, F.; Engelmann, C.; Liese, A.; Fieg, G.; Bubenheim, P.; Waluga, T. Multi-enzyme cascade reaction in a miniplant two-phase-system: Model validation and mathematical optimization. *AIChE J.* **2021**, *67*, e17158. [CrossRef]
8. Cornish-Bowden, A. *Fundamentals of Enzyme Kinetics*, 4th ed.; Completely Revised and Greatly Enlarged Edition; Wiley-Blackwell: Weinheim, Germany, 2012; ISBN 978-3-527-33074-4.
9. Sutherland, K.; Miller, C.; Bassett, A.; Cannon, J.; Cattron, E.; Escobedo, E.; Judge, K.; Hanneson, M.; Johansen, J.; Scott, D. Substrate Inhibition in Myoglobin and Hemoglobin: Kinetic Insights into Pseudo-Peroxidase Activity. *AppliedChem* **2025**, *5*, 23. [CrossRef]
10. Frère, J.-M.; Verlaine, O.; Matagne, A. The measurement of true initial rates is not always absolutely necessary to estimate enzyme kinetic parameters. *Sci. Rep.* **2023**, *13*, 15053. [CrossRef]
11. Cornish-Bowden, A. The origins of enzyme kinetics. *FEBS Lett.* **2013**, *587*, 2725–2730. [CrossRef]
12. Holzhütter, H.-G. Studying Enzyme Kinetics by Means of Progress-Curve Analysis. In Proceedings of the 1st International Beilstein Workshop, Rüdesheim, Germany, 5–8 October 2003; pp. 99–115.
13. Waluga, T.; von Ziegner, F.; Skiborowski, M. Analytical and numerical approaches to the analysis of progress curves: A methodological comparison. *Process Biochem.* **2025**, *151*, 1–13. [CrossRef]
14. von Ziegner, F.; Brauckmann, G.; Filiz, V.; Brinkmann, T.; Bubenheim, P.; Waluga, T. Debottlenecking a 2-phase multi-enzymatic cascade by an enzyme membrane reactor—Modelling and experimental validation. *Chem. Eng. Process.-Process Intensif.* **2025**, *217*, 110499. [CrossRef]
15. Goličnik, M. Exact and approximate solutions for the decades-old Michaelis-Menten equation: Progress-curve analysis through integrated rate equations. *Biochem. Mol. Biol. Educ.* **2011**, *39*, 117–125. [CrossRef]
16. Goudar, C.T.; Harris, S.K.; McInerney, M.J.; Suflita, J.M. Progress curve analysis for enzyme and microbial kinetic reactions using explicit solutions based on the Lambert W function. *J. Microbiol. Methods* **2004**, *59*, 317–326. [CrossRef] [PubMed]
17. Duggleby, R.G. Analysis of enzyme progress curves by nonlinear regression. *Methods Enzymol.* **1995**, *249*, 61–90. [CrossRef]
18. Archontoulis, S.V.; Miguez, F.E. Nonlinear Regression Models and Applications in Agricultural Research. *Agron. J.* **2015**, *107*, 786–798. [CrossRef]
19. Gutenkunst, R.N.; Waterfall, J.J.; Casey, F.P.; Brown, K.S.; Myers, C.R.; Sethna, J.P. Universally sloppy parameter sensitivities in systems biology models. *PLoS Comput. Biol.* **2007**, *3*, 1871–1878. [CrossRef] [PubMed]
20. Garcia, T.; Coteron, A.; Martinez, M.; Aracil, J. Kinetic modelling of esterification reactions catalysed by immobilized lipases. *Chem. Eng. Sci.* **1996**, *51*, 2841–2846. [CrossRef]
21. Yadav, G.D.; Devi, K. Immobilized lipase-catalysed esterification and transesterification reactions in non-aqueous media for the synthesis of tetrahydrofurfuryl butyrate: Comparison and kinetic modeling. *Chem. Eng. Sci.* **2004**, *59*, 373–383. [CrossRef]
22. Wang, Y.; Jiang, Y.; Zhou, L.; Gao, J. Enzymatic Esterification of Ammonium Lactate with Ethanol in Organic Solvent: Kinetic Study. In Proceedings of the 2010 4th International Conference on Bioinformatics and Biomedical Engineering, Chengdu, China, 18–20 June 2010; pp. 1–4. [CrossRef]
23. Yadav, G.D.; Borkar, I.V. Synthesis of n -butyl acetamide over immobilized lipase. *J. Chem. Tech. Biotech.* **2009**, *84*, 420–426. [CrossRef]
24. Fjerbaek, L.; Christensen, K.V.; Norddahl, B. A review of the current state of biodiesel production using enzymatic transesterification. *Biotechnol. Bioeng.* **2009**, *102*, 1298–1315. [CrossRef] [PubMed]
25. van Hecke, W.; Martinez-Garcia, M.; Satyawali, Y.; Porto-Carrero, C.; De Wever, H. Unraveling Lipase's Promiscuous Behavior: Insights into Organic Acid Inhibition during Solventless Ester Production. *Org. Process Res. Dev.* **2024**, *28*, 3989–4002. [CrossRef]
26. Heeres, A.; Vanbroekhoven, K.; van Hecke, W. Solvent-free lipase-catalyzed production of (meth)acrylate monomers: Experimental results and kinetic modeling. *Biochem. Eng. J.* **2019**, *142*, 162–169. [CrossRef]
27. Hong, H.; Choi, B.; Kim, J.K. Beyond the Michaelis-Menten: Bayesian Inference for Enzyme Kinetic Analysis. *Methods Mol. Biol.* **2022**, *2385*, 47–64. [CrossRef]
28. Matsui, I.; Ishikawa, K.; Matsui, E.; Miyairi, S.; Fukui, S.; Honda, K. Subsite structure of Saccharomycopsis alpha-amylase secreted from Saccharomyces cerevisiae. *J. Biochem.* **1991**, *109*, 566–569. [CrossRef]
29. Schnell, S.; Maini, P.K. Enzyme kinetics far from the standard quasi-steady-state and equilibrium approximations. *Math. Comput. Model.* **2002**, *35*, 137–144. [CrossRef]
30. Pedersen, M.G.; Bersani, A.M.; Bersani, E.; Cortese, G. The total quasi-steady-state approximation for complex enzyme reactions. *Math. Comput. Simul.* **2008**, *79*, 1010–1019. [CrossRef]
31. Kim, J.K.; Josić, K.; Bennett, M.R. The validity of quasi-steady-state approximations in discrete stochastic simulations. *Biophys. J.* **2014**, *107*, 783–793. [CrossRef]
32. Waghmare, G.V.; Chatterji, A.; Rathod, V.K. Kinetics of Enzymatic Synthesis of Cinnamyl Butyrate by Immobilized Lipase. *Appl. Biochem. Biotechnol.* **2017**, *183*, 792–806. [CrossRef]
33. Westwood, I.M.; Sim, E. Kinetic characterisation of arylamine N-acetyltransferase from Pseudomonas aeruginosa. *BMC Biochem.* **2007**, *8*, 3. [CrossRef]

34. Chaloner, K.; Verdinelli, I. Bayesian Experimental Design: A Review. *Statist. Sci.* **1995**, *10*, 273–304. [CrossRef]
35. Pronzato, L. Optimal experimental design and some related control problems. *Automatica* **2008**, *44*, 303–325. [CrossRef]
36. Zhang, D.-H.; Li, C.; Zhi, G.-Y. Kinetic and thermodynamic investigation of enzymatic L-ascorbyl acetate synthesis. *J. Biotechnol.* **2013**, *168*, 416–420. [CrossRef]
37. Stromme, J.H.; Theodorsen, L. Gamma-glutamyltransferase: Substrate inhibition, kinetic mechanism, and assay conditions. *Clin. Chem.* **1976**, *22*, 417–421. [CrossRef]
38. Picott, K.J.; Deichert, J.A.; deKemp, E.M.; Snieckus, V.; Ross, A.C. Purification and Kinetic Characterization of the Essential Condensation Enzymes Involved in Prodiginine and Tambjamine Biosynthesis. *Chembiochem* **2020**, *21*, 1036–1042. [CrossRef] [PubMed]
39. Stroberg, W.; Schnell, S. On the estimation errors of KM and V from time-course experiments using the Michaelis-Menten equation. *Biophys. Chem.* **2016**, *219*, 17–27. [CrossRef]
40. Sager, S. Sampling Decisions in Optimum Experimental Design in the Light of Pontryagin's Maximum Principle. *SIAM J. Control Optim.* **2013**, *51*, 3181–3207. [CrossRef]